Progress In Electromagnetics Research, PIER 85, 25–37, 2008

STEPPED-FREQUENCY ISAR MOTION COMPENSATION USING PARTICLE SWARM OPTIMIZATION WITH AN ISLAND MODEL

S. H. Park and H. T. Kim

Department of Electronic and Electrical Engineering
Pohang University of Science and Technology (POSTECH)
San 31, Hyoja-Dong, Nam-Ku, Pohang, Kyoung-buk, 790-784, Korea

K. T. Kim

School of Electrical Engineering and Computer Science
Yeungnam University
214-1, Dae-Dong, Gyeongsan-si, Kyungbuk 712-749, Korea

Abstract—This paper proposes a motion compensation method to compensate for the inter-pulse phase errors caused by the target movement in stepped-frequency ISAR imaging. For this purpose, genetic algorithm, particle swarm optimization (PSO) and PSO with an island model (PSOI) were applied in the proposed procedure. Simulation results using point scatterers and measured data show that PSOI is the most efficient in the proposed method.

1. INTRODUCTION

Inverse Synthetic Aperture Radar (ISAR) imaging is a technique to generate a two-dimensional image of a target [1]. ISAR is used as a good feature along with 1D range profile [2] in automatic target recognition (ATR). There are two main types for deriving ISAR images; chirp pulse radar and stepped-frequency radar (Fig. 1(a)).

Chirp pulse radar, widely used in imaging radars, transmits a single short pulse with a given bandwidth. The returned signal is matched-filtered using a stored replica. It is assumed that the target is fixed during the dwell time of the pulse on it due to a relatively short pulse length compared with its speed. Therefore, range profile time-history data calculated by the chirp pulse radar remain well-focused.

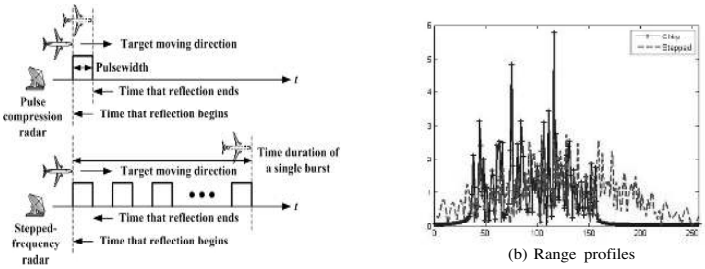

(a) Imaging mechanism (b) Range profiles

Figure 1. Comparison of chirp and stepped-frequency radars.

However, this type of radar is often limited by hardware complexity and cost.

Stepped-frequency radar system transmits a continuous series of short monotone pulses, called burst with only a single frequency component in each pulse. The inverse Fourier transform (IFFT) of each burst is used to generate each range profile. Stepped-frequency radar can achieve high resolution even with simple hardware architecture. However, the motion of the target between pulses in a burst can blur the range profile seriously (Fig. 1(b)). Some papers for autofocusing stepped-frequency ISAR images have been published, but assumed that target's movement is negligible during a single burst [3].

In this paper, we propose a stepped-frequency motion compensation procedure that compensates for such inter-pulse motion of a target. For this purpose, a genetic algorithm (GA) [4], a particle swarm optimization (PSO) [5–9], a PSO with an island model (PSOI) [10] were utilized in each stepped-frequency burst using 1D entropy cost function. Simulation results using a target composed of point scatterers and the measured signal of Boeing 737 aircraft show PSOI compensates for the phase errors most successfully.

2. RADAR SIGNAL MODEL AND PROPOSED MOTION COMPENSATION METHOD

2.1. Stepped-Frequency Signal Model

A stepped-frequency signal burst consists of M bursts of N pulses whose pulse repetition frequency (PRF) is $1/T$ (Fig. 2). Each frequency component in the burst is $f_n = f_0 + n\Delta f$, where f_0 is the initial frequency and Δf is the frequency step in the burst, yielding the total bandwidth of $(N-1)\Delta f$. We assumed that the radar line-of-sight

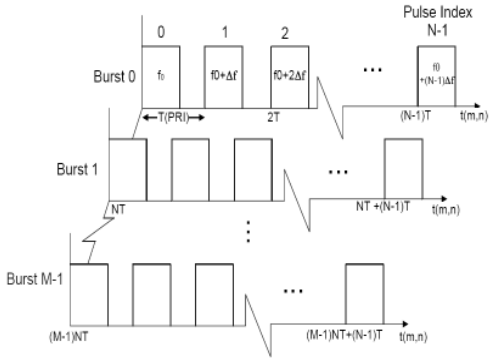

Figure 2. Stepped frequency waveform.

(RLOS) is fixed during each burst. The received stepped-frequency echo signal can be expressed as follows:

$$\begin{aligned} s(m,n) &= \sum_{k=1}^{K} a_k exp\left[-j\frac{4\pi f_n}{c} r_k(m,n)\right] \\ r_k(m,n) &= r_{k0}(m) + v_r(m)t_n + \frac{1}{2}a_r(m)t_n^2 \end{aligned} \tag{1}$$

where K is the number of scattering centers, a_k is the magnitude of the kth scattering center, and $r_k(m,n)$ is the radial distance to kth scattering center projected onto RLOS at the time $mT + nT$, $r_{k0}(m)$ is the initial radial distance of the kth scattering center at the start of the mth burst, and $t_n = nT$. V_r and a_r respectively represent the velocity and acceleration along RLOS.

In (1), a change of r_k between pulses causes the image to be blurred. Therefore this blurring should be eliminated by using proper estimation of $\hat{v_r}$ and $\hat{a_r}$ in each burst. The compensated signal is then as follows:

$$\begin{aligned} s'(m,n) &= s(m,n) \times \exp\left(j\frac{4\pi f_n}{c}[\hat{v_r}(m)t_n + \frac{1}{2}\hat{a_r}(m)t_n^2]\right) \\ &= \sum_{k=1}^{K} a_k \exp\Bigg(- j\frac{4\pi f_n}{c}\big[r_{k0}(m) + (v_r(m) - \hat{v_r}(m))t_n \\ &\quad + \frac{1}{2}(a_r(m) - \hat{a_r}(m))t_n^2\big]\Bigg) \end{aligned} \tag{2}$$

After (2) is calculated, scattering centers in each burst are at fixed locations, yielding a focused range profile when IFFT is performed.

However, phase errors for each range burst still exist due to $r_{k0}(m)$ of each burst. For this reason, range profiles should be aligned using proper range alignment algorithm.

2.2. Proposed Motion Compensation Method

To properly compensate the motion of the target during each burst by estimating $\hat{v_r}$ and $\hat{a_r}$, we utilize a one-dimensional (1D) entropy minimization method in which 1D entropy is used as the cost function that quantifies the focus of a range profile. It is defined as follows [12, 13]:

$$Ent = -\sum_{n=1}^{N-1} h(n) \ln h(n) \tag{3}$$

where $h(n)$ is the range profile derived via IFFT of a motion-compensated burst. The estimated set of $[\hat{v_r}\ \hat{a_r}]$ that minimizes this cost function is selected as the one for motion compensation of the burst.

However, finding $[\hat{v_r}\ \hat{a_r}]$ is not simple because the cost surface is composed of many local minima. Therefore, gradient-based searching algorithms, which are faster than any other methods, can yield poorly focused range profiles. In this paper, we utilize GA, PSO, and PSOI. To reduce the computation time which is the crucial factor in battlefield conditions, we limit the number of generations in each method to 30 and then evaluate the degree of focus using each algorithm.

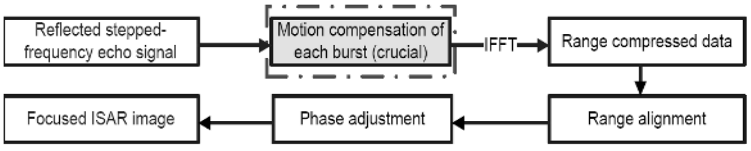

Figure 3. Proposed motion compensation procedure.

After proper motion compensation of each burst, we used range alignment of each range profile using 1D entropy minimization and phase adjustment using 2D entropy minimization to align range profiles due to the intial radial distance at each burst and to compensate for the phase errors in cross-range direction. Fig. 3 shows the proposed procedure for stepped-frequency ISAR imaging. Without the highlighted step, ISAR images derived from stepped-frequency can be blurred seriously due to the inter-pulse motion of the target, especially at high target speeds (dotted line in Fig. 1(b)).

2.3. GA, PSO and PSOI

GAs are a class of robust optimization methods modeled on the concepts of natural selection and evolution. GAs are adept at handling complex, multi-modal optimization problems, particularly those that are naturally combinatorial.

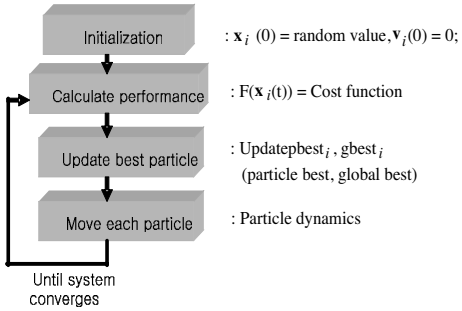

Figure 4. Principle of PSO method.

PSO is a population based stochastic optimization technique based on social behavior of bird flocking or fish schooling. The system is initialized with a population of random solutions, called particles, that minimizes the cost function and searches for the optima by changing the velocity of each particle toward the local and the global particle best (Fig. 4) [6]. The particle dynamics which update each particle is as follows:

$$\begin{aligned} &\vec{v_i}(t) = \phi\vec{v_i}(t-1) + \rho_1(\vec{x_{pbest}} - \vec{x_i}(t)) + \rho_2(\vec{x_{gbest}} - \vec{x_i}(t)) \\ &\text{where, } \rho_1 = r_1c_1,\ \rho_2 = r_2c_2,\ r_1, r_2 \approx rand,\ c_1, c_2 > 0\ , c_1 + c_2 < 4 \end{aligned} \tag{4}$$

t is the number of generation, rand is a uniform random number having a uniform distribution between 0 and 1. The velocity vector in the tth generation is then added to the particle $\vec{x_i}(t)$ to move this particle. It was demonstrated that PSO gets better results in a faster, cheaper way compared with other methods [12]. Another reason for using PSO is that there are few parameters to adjust (c_1, c_2, and ϕ).

In this paper, along with PSO alone, a PSOI model that combines three independent PSOs were designed to further increase the performance of PSO in motion compensation. This concept in Fig. 5 was designed by modifying the structure given in reference [10] to reduce computation time. For every regular generation step, two particles with the poorest performance in each subpopulation are discarded and two best particles of the other two PSOs, one from each subpopulation, are migrated. Therefore, each subpopulation

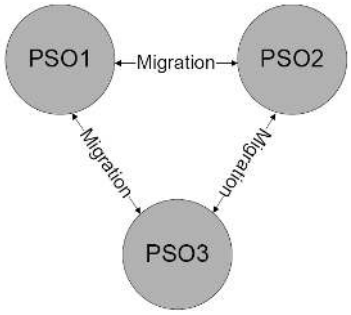

Figure 5. PSOI.

cooperates to find the optimum value. There can be many subpopulations, however, we limited the number to three because of the calculation speed constraints.

3. SIMULATION RESULT

3.1. Simulation Result Using Point Scatterers

Stepped-frequency ISAR simulation was conducted for moving targets (Fig. 6(a)) which was composed of isotropic scattering centers (Fig. 6(b)). The magnitude of all scatterers was set to identically two.

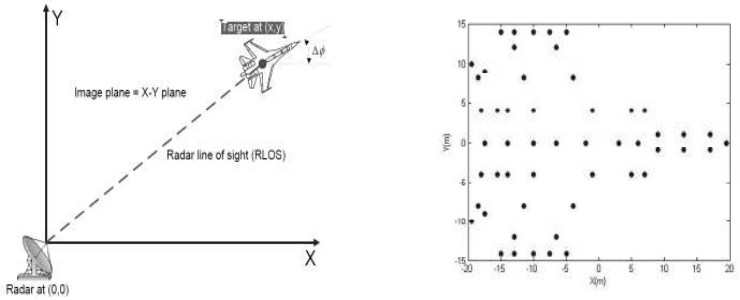

(a) Geometry (b) Target

Figure 6. The geometry for ISAR imaging and the target used

In this figure, $\Delta\phi$ was set to zero for simplicity. The simulation was carried under the given radar and motion parameters (Table 1) and GA, PSO, PSOI parameters (Table 2). The velocity and the

Table 1. Radar and motion parameters.

PRF	5kHz	Initial position	[30,30,0](km)
Start frequency	9GHz	Velocity vector	[300,0, 0](m/s)
Bandwidth	512MHz	Acceleration vector	[20,0,0](m/s^2)
No. of pulses	256	No. of bursts	64

Table 2. GA, PSO, PSOI parameters.

GA		Population size	Cross over rate	Mutation rate	Crossover and Selection
		30	0.83	0.03	One point and roulette wheel
PSO		Population size	Inertia weight	C1	C2
		30	0.61	1.45	1.51
PSOI	PSO1	10	0.58	1.47	1.51
	PSO2	10	0.62	1.48	1.47
	PSO3	10	0.57	1.44	1.48

Table 3. Avg and std of the minimum entropy and avg computation time.

	GA	PSO	PSOI
Minimum entropy	3.5865	3.4665	3.4415
Standard deviation	0.01408	0.0305	0.0044
Average computation time (sec)	0.1694	0.2435	0.2485

acceleration were selected to simulate an accelerating fighter, which is coming to attack. To determine the parameters in each algorithm, 5 simulations were performed varying each parameter and those that yielded best average results were selected.

To save computation time which is the most important factor in the real ATR situation, the population size of each algorithm was set to 30 and the number of generations was fixed at 30. Fig. 7 shows the cost surface of the first range profile of the target. It is composed of many local minima.

Fig. 8 shows the evolution curve for each algorithm to focus the 1st range profile and the focused range profiles along with the unfocused one. It can be seen that each method focuses the unfocused range profile successfully. Table 3 shows the average and the standard

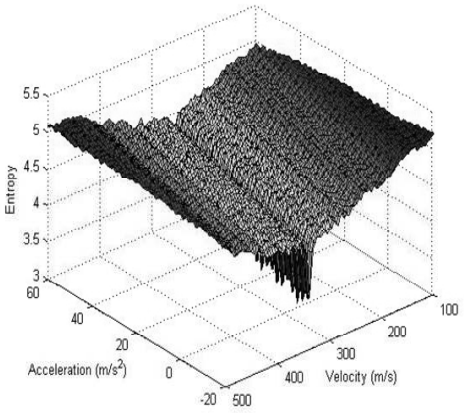

Figure 7. The cost surface of the 1st range profile.

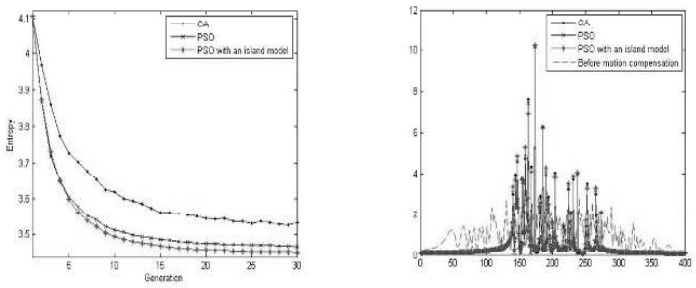

(a) Evolution curve (b) Focused range profiles

Figure 8. Comparison of evolution curve and focused range profiles

deviation of the minimum entropy and the average computation time of each algorithm. Intel QuadCore processor was used for the computation. Each algorithm was carried out 100 times using the same random initial population each time. The range of velocity was $100 \sim 500\,\mathrm{m/s}$ and that of acceleration was $-10 \sim 70\,\mathrm{m/s^2}$.

The minimum entropy of each method decreased as the number of generations increased (Fig. 8). The average and the standard deviation of the minimum entropy were smallest for PSOI (Table 3). PSO outperforms GA in the aspect of accuracy in the fixed short evolution time and its standard deviation is less stable than GA. The average computation time of PSO and PSOI was slightly longer due to searching for the global best and the particle best. However, this

doesn't mean GA is faster than PSO in finding the optimum solution because more time is required for GA to obtain the same result as PSO and PSOI.

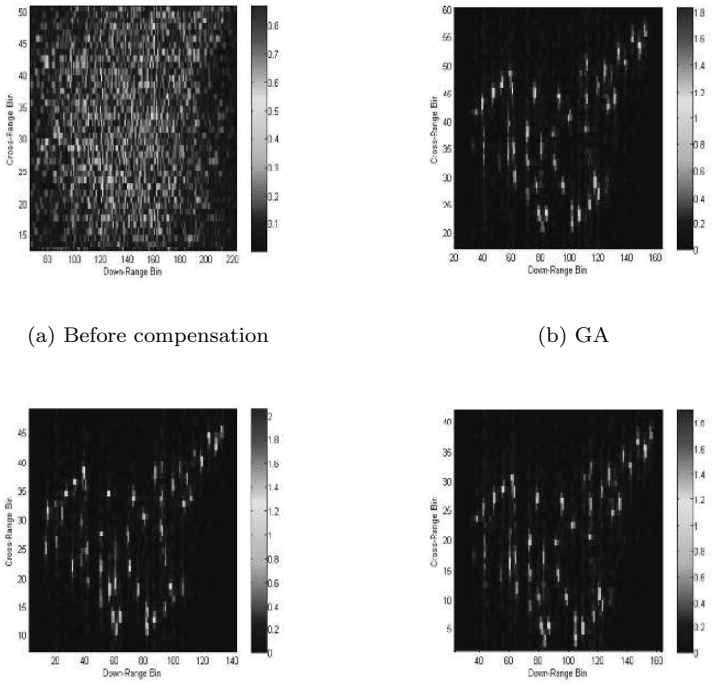

(a) Before compensation (b) GA

(c) PSO (d) PSOI

Figure 9. ISAR images focused by each result.

Figure 9 shows ISAR images focused by each method and Table 4 shows the average and the standard deviation of 2D entropy and the average computation time for 100 independent simulations. 2D entropy is defined as follows [13–15]:

$$H_e(I) = -\sum_{m=0}^{M-1}\sum_{n=0}^{N-1} \bar{I}(m,n)\ln \bar{I}(m,n),$$
$$\text{where, } \bar{I}(m,n) = \frac{|I(m,n)|^2}{\sum_{m=0}^{M-1}\sum_{n=0}^{N-1}|I(m,n)|^2} \tag{5}$$

Table 4. Avg and std of the minimum entropy and avg computation time.

	GA	PSO	PSOI
Minimum entropy	6.3236	6.2045	6.1657
Std (entropy)	0.0795	0.1098	0.0298
Avg computation time (sec)	9.7248	12.5412	13.2457

According to this criterion, the image having the minimum entropy is the most successfully focused. Even though more time was consumed to iterate a fixed evolution number, PSOI shows the best performance (Table 4) in the aspect of the image focus because ISAR images are just 2D extensions of 1D range profiles. For GA to derive the same result, it has to evolve more and this will increase the computation time further.

3.2. Simulation Result Using Measured ISAR Data

In Section 3.1, PSOI compensated the motion most successfully. In this section, we demonstrate the performance of PSOI using the measured ISAR image of a Boeing 737 aircraft in flight. The raw data for this image were obtained using a chirp waveform. The bandwidth of the radar was 100 Mhz, corresponding to a 1.5 m down-range resolution. The complex ISAR image was transformed into stepped-frequency domain via FFT. Then for each frequency data at a certain aspect angle, $v_r = 300\,\mathrm{m/s}$ and $a_r = 20\,\mathrm{m/s^2}$ were added as follows:

$$z_n = y_n \times \left(-j \frac{4\pi f_n}{c} \left(v_r t_n + \frac{1}{2} a_r t_n^2 \right) \right), \quad n = 1, 2, \ldots, N \tag{6}$$

where y_n is the frequency domain data of a range profile and z_n is the nth motion-added frequency data of it. All other parameters are the same as in (1).

Figure 10(a) shows the original image derived by chirp waveform and (b), (c) shows the images before and after motion compensation in stepped frequency waveform. Comparison of Fig. 10(a) and Fig. 10(c) demonstrates that PSOI is very effective in motion compensation of stepped-frequency ISAR images, even for the measured data.

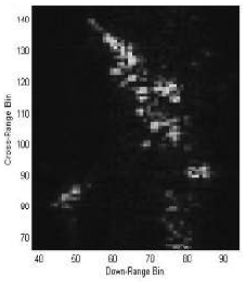

(a) ISAR image by chirp waveform

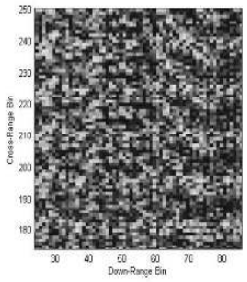

(b) Before motion compensation

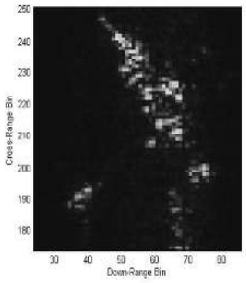

(c) After motion compensation

Figure 10. ISAR images obtained by the measured data.

4. CONCLUSION

In this paper, we proposed a stepped-frequency motion compensation procedure that successfully compensated for the phase errors caused by the motion of a target between pulses in a burst. Simulation results using a target composed of point scatterers as well as the measured data proved the efficiency of this motion compensation method. In the estimation of motion parameters, PSOI provided the most accurate and stable image focus.

REFERENCES

1. Chen, C. C. and H. C. Andrews, "Target-motion-induced radar imaging," *IEEE Trans. Aerospace and Electronic Systems*, Vol. 16,

No. 1, 2–14, Jan. 1980.

2. Park, S.-H., K.-K. Park, J.-H. Jung, H.-T. Kim, and K.-T. Kim, "Construction of training database based on high frequency RCS prediction methods for ATR," *Journal of Electromagnetic Waves and Applications*, Vol. 22, 693–703, 2008.
3. Li, J., R. Wu, and V. C. Chen, "Robust autofocus algorithm for ISAR imaging of moving targets," *IEEE Trans. Antennas Propagat.*, Vol. 37, No. 3, 1056–1069, 2001.
4. Holland, J. H., *Adaptation in Natural and Artificial Systems*, The University of Michigan Press, Michigan, 1975.
5. Eberhart, R. C. and J. Kennedy, "A new optimizer using particle swarm theory," *Proceedings of the Sixth International Symposium on Micro Machine and Human Science*, 39–43, Nagoya, Japan, 1995.
6. Kennedy, J. and R. C. Eberhart, *Swarm Intelligence*, Academic Press, 2001.
7. Koo, V. C., Y. K. Chan, and H. T. Chuah, "Multiple phase difference method for real-time SAR autofocus," *J. of Electromagn. Waves and Appl.*, Vol. 20, No. 3, 375–388, 2006.
8. Lim, T. S., V. C. Koo, H. T. Ewe, and H. T. Chuah, "High-frequency phase error reduction in SAR using particle swarm of optimization algorithm," *J. of Electromagn. Waves and Appl.*, Vol. 21, No. 6, 795–810, 2007.
9. Lim, T. S., V. C. Koo, H. T. Ewe, and H. T. Chuah, "A SAR autofocus algorithm based on particle swarm optimization," *Progress In Electromagnetics Research B*, Vol. 1, 159–176, 2008.
10. Huang, D. S., X.-P. Zhang, and G.-B. Huang, "Reconstruction of superquadric 3D models by parallel particle swarm optimization algorithm with island model," *ICIC 2005*, Part I, LNCS 3644, 757–766, Apr. 2005.
11. Li, X., G. Liu, and J. Ni, "Autofocusing of ISAR images based on entropy minimization," *IEEE Trans. Aerospace and Electronic Systems*, Vol. 35, No. 4, 1240–1251, Oct. 1999.
12. Hassan, R., B. Cohanim, and O. Weck, "A comparison of particle swarm optimization and the genetic algorithm," *46th AIAA/ASME/ASCE/AHS/ASC Structures, Structural Dynamics & Materials Conference*, 18–21, Apr. 2005.
13. Wang, J., X. Liu, and Z. Zou, "Minimum-entropy phase adjustment for ISAR," *IEE Proc. Radar Sonar Navig.*, Vol. 151, No. 4, 203–209, Aug. 2004.
14. Lazarov, A. and C. Minchev, "ISAR signal modeling and image

reconstruction with entropy minimization autofocusing," *Proc. DASC 2006*, 1–11, Portland, USA, Oct. 17–19, 2006.

15. Karakasiliotis, A. V., A. D. Lazarov, P. V. Frangos, G. Boultadakis, and G. Kalognomos, "Two-dimensional ISAR model and image reconstruction with stepped frequency modulated signal," accepted for publication in *IET Signal Processing Journal, Special Issue on ISAR Signal Processing Techniques and Feature Extraction*, April 2008.

Errata to STEPPED-FREQUENCY ISAR MOTION COMPENSATION USING PARTICLE SWARM OPTIMIZATION WITH AN ISLAND MODEL

by S.-H. Park, H.-T. Kim, and K.-T. Kim, in *Progress In Electromagnetics Research*, PIER 85, pp. 25–37, 2008

(1) Line 21 in page 29 ∼ line 1 in page 30: The paragraph

In this paper, along with PSO alone, a PSOI model that combines three independent PSOs were designed to further increase the performance of PSO in motion compensation. This concept in Fig. 5 was designed by modifying the structure given in reference [10] to reduce computation time. For every regular generation step, two particles with the poorest performance in each subpopulation are discarded and two best particles of the other two PSOs, one from each subpopulation, are migrated. Therefore, each subpopulation cooperates to find the optimum value. There can be many subpopulations, however, we limited the number to three because of the calculation speed constraints.

should be changed to

In this paper, along with PSO alone, a PSOI model that combines three independent PSOs were applied to further increase the performance of PSO in motion compensation. Fig. 5 shows the concept of PSOI proposed in [10] to improve the performance of PSO. The evolution in subpopulation is performed by a stand-alone sub-process and each sub-process periodically sends the best particle of it to the main process. Then the main process selects the global best and sends it back to each subpopulation. This operation guides each subpopulation to the global best. There can be many subpopulations. However, we selected only three subpopulations because of the computation time.

(2) Fig. 5 in page 30 must be changed to

2

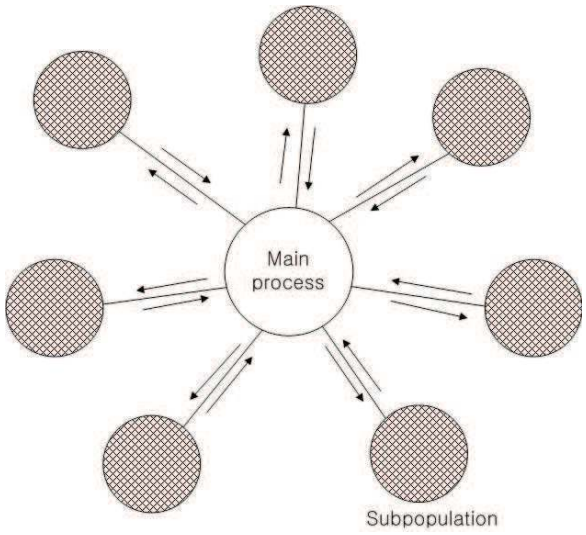

(3) Table 3 must be changed from

	GA	PSO	PSOI
Minimum entropy	3.5865	3.4665	3.4415
Standard deviation	0.01408	0.0305	0.0044
Average computation time (sec)	0.1694	0.2435	0.2485

to

	GA	PSO	PSOI
Minimum entropy	3.5865	3.4665	3.4511
Standard deviation (entropy)	0.01408	0.0305	0.0052
Average computation time (sec)	0.1694	0.2435	0.2533

(4) Table 4 must be changed from

	GA	PSO	PSOI
Minimum entropy	6.3236	6.2045	6.1657
Standard deviation (entropy)	0.0795	0.1098	0.0298
Avg computation time (sec)	9.7248	12.5412	13.2457

to

	GA	PSO	PSOI
Minimum entropy	6.3236	6.2045	6.1731
Standard deviation (entropy)	0.0795	0.1098	0.0345
Avg computation time (sec)	9.7248	12.5412	13.1288